Ashbourn, J. M. A. and Woods, L. C. and Bingham, R. (2001) Heating plasma loops in the solar corona. Astrophysical Journal, 553 (2). pp. 941-948. ISSN 0004-637X , http://dx.doi.org/10.1086/320956

This version is available at http://strathprints.strath.ac.uk/51970/

THE ASTROPHYSICAL JOURNAL, 553:941–948, 2001 June 1

HEATING PLASMA LOOPS IN THE SOLAR CORONA

J. M. A. ASHBOURN AND L. C. WOODS
Mathematical Institute, University of Oxford, 24-29 St. Giles', Oxford, OX1 3LB, England, UK; j.m.a.ashbourn@damtp.cam.ac.uk, leslie.woods@balliol.oxford.ac.uk

AND

R. BINGHAM
Rutherford Appleton Laboratory, Chilton, Didcot, Oxford, OX11 0QX, England, UK; r.bingham@rl.ac.uk
Received 2000 August 25; accepted 2001 February 7

ABSTRACT

We find a new heat source term for hot coronal loops and include it in the energy equation. This term requires the loop to be hotter than the ambient corona and depends on the combined effect of electron fluid shear and the temperature gradient. Under certain circumstances, the shear drives the heat up the radial temperature gradient into a cross section of the magnetic flux tube from which it leaves by radiation and by conduction down the axial temperature gradient in the usual manner. The heat source is thus a surface term applied over the whole of the loop rather than a volume-distributed term, and its strength is proportional to the cube of the temperature. We apply it to the usual scaling law and obtain an expression for the radius of the flux tube for thermal equilibrium to hold. The temperature distribution around the plasma loop is determined and compared with recent observations and is found to be in satisfactory agreement with them.

Subject headings: MHD — plasmas — Sun: corona

1. INTRODUCTION

A central problem with modeling the hot coronal plasma loops, which may reach heights of 50,000 km or more, is that of finding how they are heated. These loops sometimes persist for days, which is long enough to validate steady state models; hence, losses due to thermal conduction and radiation need to be balanced by a supply of thermal energy, but finding a convincing heating mechanism has proved elusive. In most theories, it is assumed that the energy comes from regions below the photosphere, with the magnetic field playing an important role in the transport and dissipation of this energy. But since all of the coronal energy must in some way or another find its way from these regions, this is almost self-evident. Our present concern is not with the problem of heating the whole corona but with the heating of the hot plasma loops, some of which can be orders of magnitude hotter than the ambient plasma. Bray et al. (1991) give a useful brief survey based on Wentzel's (1981) review.

Zirker (1993) reviews the basic suggested mechanisms—wave heating, turbulence, electric currents, and reconnection—and concludes that all are possible. The upward propagation of MHD waves generated by footpoint motions is one of the mechanisms proposed for the heating of loops. Apart from fast MHD waves, which cannot penetrate the corona, the slow modes and the Alfvén modes can deposit energy into the loops, especially if mode coupling is included in the process. If it were assumed that the dissipation of waves propagating up from the photosphere energy were responsible for the heating, this energy would be supplied close to the base of the loops. Heyvaerts & Priest (1983) have considered the possibility that standing waves already present in the loops and being reflected at the footpoints could heat the loops by the phase mixing that is inevitable in strong temperature gradients, a process that would result in a distribution of heating along the whole of the loop. Foukal & Hinata (1977) believe that there could be another mechanism for heating loops, suggesting that such structures are not heated irreversibly but that the observed radiation losses could be balanced by extracting energy from a nearby reservoir. In fact, this speculation agrees with the model that we shall describe in this paper (the "reservoir" being the corona in the neighborhood of the loop); although as with all heat transport, the process is not strictly irreversible.

Joule heating is a mechanism that has received much attention, but it is found that an enormous total current and large poloidal field result unless the plasma loop is fragmented into a large number of filaments. The dissipation occurs in boundary strips of width $\delta_B = B(\mu_0 j)$, where j is the current density, B is the magnetic field strength, and μ_0 is the permeability. (We have adopted SI units unless indicated otherwise.) If electron drift speeds reach the ion sound speed, j attains its maximum value j_m, in which case the strips are typically less than a kilometer wide ($\delta_B \sim 3.5 \times 10^4 B$; see eq. [18]). Ion-acoustic waves are generated, which in turn scatter and heat the electrons (Hinata 1979). However, the scattering amounts to an increase in the electron collision frequency and hence to an increase in the electrical resistivity, which reduces the current and hence switches off the instability. The drift speed can now increase to the limit again, so conditions switch back and forth between weak turbulence and classical conditions, keeping the process in marginal stability.

The ohmic heating rate ηj_m^2 occurs in a volume $2\pi RL\delta_B$, where R is the radius of the flux loop and L is its length, and it can therefore balance a radiation loss rate of $\mathscr{L} \sim \eta j_m^2(2\delta_B/R)$ per unit volume. At the typical value of $T = 10^6$ K, we find that $\eta j_m^2 \sim 10^{-3}$ W m^{-3} and $\mathscr{L} \sim 10^{-4}$ W m^{-3} (see eq. [23]), so for ohmic heating to be marginally adequate—we are ignoring conduction losses, which would make the situation worse—we must have $R < 20\delta_B$. We therefore need a mechanism capable of fragmenting the flux tube into threads of less than about 20 km in radius. Another kind of fragmentation that could resolve the problem of ohmic heating is to suppose that current sheets form in the flux tube. For example, one could image nested annuli in each of which the magnetic field orientation is different from its neighboring shells. While this would certainly enlarge the volume of the ohmically heated regions, the nested field structure would be difficult to generate even by swirling motions at the footpoints of the loops, and there is the added difficulty that the heating rate would be too slow. Bray et al. (1991) give an account of the model and provide a number of references.

Another much favored and related dissipative process is the reconnection of sheared field lines with the aid of the tearing-mode instability, provided this occurs in a plasma flow strongly converging toward the neutral points in the magnetic field, a process known as "flux pileup." The difficulty with this model is that for the rate of heating to reach the values implied by observation, the flow must convergence with velocities of at least 1% of the Alfvén speed, which in loops with a field of about 100 G is $\sim 3 \times 10^3$ km s^{-1}. Litvinenko (1999) observes that the actual rate of pileup, which is limited by either the plasma or the magnetic pressure in the pileup region, is some 3 orders of magnitude too small to explain the most powerful flares but allows that the rate may be sufficient to provide a steady source of energy to heat the persisting coronal loops. However, to require the existence of two distinct heating mechanisms depending on the rate of change of the observed phenomena is unconvincing, since while there may be isolated instances of plasma flows capable of compressing opposing field lines at speeds of 30 km s^{-1}, as a general phenomenon high in the corona, it seems unlikely.

If s denotes the distance measured along a loop, then the temperature distribution, $T(s)$, can be deduced from observations; Priest et al. (1998) have used such observations to deduce an important characteristic of the heating process, at least for certain types of loops. When they adopted a standard model of a loop and supplied the heat with (*a*) a maximum at the bottom of the loop that is decaying exponentially over a distance a small fraction of the length of the loop, (*b*) a heat source at the loop summit, and (*c*) heating uniformly distributed over the loop, they found modest agreement between the theory and the observations for case *b* and better still agreement with case *c*, whereas case *a* was statistically very unlikely. Neupert, Nakagawa, & Rust (1975) concluded from their observations that models in which energy is only supplied at the base of a flux tube were inappropriate for loops over active regions; thus, the observations would seem to be consistent with a distributed heating source that has a maximum at the summit, a property of the mechanism that we shall advance below. However, recent studies of active region loops observed with the *Transition Region and Coronal Explorer* (*TRACE*) by Aschwanden, Nightingale, & Alexander (2000) appear to give strong support for a heat source concentrated near the bottom of the loop, but as the authors point out, their collection of loops are both cooler and larger than those considered by Priest et al. (1998).

Galsgaard et al. (1999) used a numerical experiment to generate flux braiding that in turn generated electric current concentrations and Joule heating. They found that they were able to obtain good approximations to each of the three types of heating described above, and with the constraint that the total heating was the same in each case, they obtained a number of similar distributions with small variations in the magnitude of the temperature at the summit of the loop. These changes depended on the type of boundary conditions applied at each end of the loop and on the choice of the distribution of heating along the loop. Unfortunately, the temperature variations were only a little larger than the errors in present observations, so as a means of discriminating between various heating mechanisms, their use is inconclusive.

Any heating mechanism must meet the overall energy constraint, namely, that the energy it supplies the whole loop at least equals the energy lost by radiation. This can be represented by Q_b W m^{-2}, where Q_b is the heat flux that must be fed into the base of the loop, although the actual heating mechanism need not have this physical origin. Svestka et al. (1977) give an observational estimate of $Q_b = 7 \times 10^2$ W m^{-2}.

There is one important feature of a loop that distinguishes it from other coronal structures, namely, its finite total length $2L$. In models of plasma loops, it is usually assumed that the pressure p in the loop is constant and that the maximum temperature of the loop, T_m, occurs at the apex of the loop; it was demonstrated by Rosner, Tucker, & Vaiana (1978) and by Craig, McClymont, & Underwood (1978) that a relationship must exist between the length of a loop and its thermodynamic properties. One form of this relationship, known as a scaling law, is $pL = aT_m^{\alpha}$, where a and α are constants depending on which radiation and heating laws are adopted. But while a satisfactory approximation to the radiation rate is known, at present the heating rate can only be a matter of speculation. It is the aim of this paper to fill this gap in the theory and as far as possible to test the outcome against observations.

The active region loops observed with *TRACE* appear to have an almost isothermal appearance, and to explain these Reale & Peres (2000) proposed that a coronal loop is actually a synthesis of many loop threads, each of which satisfies a steady state scaling law of the Rosner et al. (1978) type (the RTV theory). By adopting a logarithmic distribution of the maximum temperatures of the threads, they were able to model these near-isothermal *TRACE* loops. Aschwanden et al. (2000) adopted this model too and extended it to analyze their observations of a collection of large, relatively cool loops. They found that it was necessary to heat the threads near their base in order to bring their semiempirical theory into agreement with the observations, and in an extension of this work, Aschwanden, Schrijver, & Alexander (2001) have calculated a large number of hydrostatic solutions appropriate for large loops, from which they show that only nonuniform heating concentrated near the base of the loop was consistent with the observations.

2. THE SECOND-ORDER HEATING MECHANISM, WITH NO MAGNETIC FIELD

First, we shall deal with the case when there is no magnetic field, since the result can then easily be extended to cover the case of a strong magnetic field. When the Chapman-Enskog expansion in powers of the Knudsen number ϵ is applied to Boltzmann's kinetic equation, the resulting formula for the heat flux vector $\boldsymbol{q}$ takes the form $\boldsymbol{q} = \boldsymbol{q}_1 + \boldsymbol{q}_2 + O(\epsilon^3)$, where $\boldsymbol{q}_1$ is the classical Fourier expression $\boldsymbol{q}_1 = -\kappa \nabla T$ and $\boldsymbol{q}_2$ is the second-order heat flux, which for a neutral gas is usually attributed to Burnett (1935a, 1935b). Starting from $\boldsymbol{q}_1$, we first give a physical derivation of $\boldsymbol{q}_2$ and then extend the theory to magnetoplasmas. For a full treatment, see Woods (1993, 1996).

We shall adopt the following notations: $D = \partial/\partial t + \boldsymbol{v} \cdot \nabla$ for the material time derivative, $\dot{\mathbf{e}}$ for the deviator of the symmetric part $\mathbf{e}$ of the velocity gradient tensor $\nabla \boldsymbol{v}$, and $D^*\boldsymbol{q}_1 = D\boldsymbol{q}_1 - \boldsymbol{\Omega} \times \boldsymbol{q}_1$ for the material derivative in a frame convected with the fluid and spinning with an angular velocity $\boldsymbol{\Omega} = \frac{1}{2}\nabla \times \boldsymbol{v}$. (This spin is necessary to remove all ordered particle motions from the fluid element under consideration.) Our first step is to show that in the absence of a magnetic field,

$$\tau D^*\boldsymbol{q} + \boldsymbol{q} = \boldsymbol{q}_1 - \tau \dot{\mathbf{e}} \cdot \boldsymbol{q}_1 + O(\epsilon^3) \quad (\boldsymbol{q}_1 = -\kappa \nabla T) , \quad (1)$$

where τ is the microscopic relaxation time—usually the collision interval between particles of the species, electrons, or ions under consideration.

Let $\mathbf{P}$ denote the local thermodynamic system in which we wish to determine the diffusion of heat. Diffusion is the transport of a property by the purely *random* component of molecular motion. We separate diffusion from convection by noting that unlike convection, diffusion is independent of the choice of reference frame in which the fluid velocity is measured; thus, "frame indifference" is the essential property that distinguishes diffusion from convection. Not only must $\mathbf{P}$ be moving with the fluid velocity $\boldsymbol{v}$ to eliminate all ordered particle motions from $\mathbf{P}$, it must also have the *acceleration* and *spin* of the fluid element in question. The heat flux vector $\boldsymbol{q}$ must be determined relative to $\mathbf{P}$. It is also important to distinguish between *energy* flux, which does not involve collisions, and *heat* flux, which does. With the former, changing conditions at $\mathbf{P}$ plays no part, whereas with heat, collisions in $\mathbf{P}$ transform energy flux into heat. The ratio of the particle collision interval τ to the timescale $\mathscr{T}$ for appreciable changes in the macroscopic variables, namely, the Knudsen number ϵ, plays a dominant role in transport, and for the theory to be valid here, we require that $\epsilon \ll 1$.

In the laboratory frame, the system $\mathbf{P}$ has an angular velocity $\boldsymbol{\Omega} = \frac{1}{2}\nabla \times \boldsymbol{v}$; therefore, the rate of change of a vector $\boldsymbol{A}$ in $\mathbf{P}$ is given by $D^*\boldsymbol{A} \equiv D\boldsymbol{A} - \boldsymbol{\Omega} \times \boldsymbol{A}$. The only frame-indifferent vectorial terms that we can form using ∇T, the fluid velocity $\boldsymbol{v}$ and the frame-indifferent operators D^* and ∇, are $D^*\nabla T$ and $\boldsymbol{e} \cdot \nabla T$. Thus, we know what terms should appear in $\boldsymbol{q}_2$, and it remains to determine the mechanism that produces them. The first-order flux $\boldsymbol{q}_1$ has a special role in the theory. Being proportional to ∇T, it depends on distant boundary conditions, where heat is supplied or removed from the system. With these conditions held constant, $\boldsymbol{q}_1$ is the "equilibrium" value of $\boldsymbol{q} = \boldsymbol{q}_1 + \boldsymbol{q}_2 + \ldots$, with $\boldsymbol{q}_2$ being a perturbation that is due to time delays, as we shall explain below.

Let λ denote an infinitesimal vector, about a mean free path in length, which is embedded in the thermodynamic system $\mathbf{P}$. As $\mathbf{P}$ accelerates and spins relative to the laboratory frame, so does $\boldsymbol{\lambda}$. This vector therefore tags the system $\mathbf{P}$ in which the heat flux $\boldsymbol{q}$ is measured, its size and orientation being arbitrary. Thus, $\boldsymbol{\lambda}$ is a generic tag representing the environment $\mathbf{P}$ in which $\boldsymbol{q}$ is generated, and since $\boldsymbol{q}$ is the collisional deposition of energy, there is a delay time of a collision interval τ between changes in $\mathbf{P}$ and the response in $\boldsymbol{q}$. As $\mathbf{P}$ is represented by the tag $\boldsymbol{\lambda}$, for a given value of $\boldsymbol{q}$ at time t, it is necessary to characterize the environment by the value of $\boldsymbol{\lambda}$ at a time τ earlier than the present time.

Let $\boldsymbol{\lambda}_\tau$ denote the value of $\boldsymbol{\lambda}$ at time $(t - \tau)$, then the *relative* heat flux is defined by

$$\xi \equiv \boldsymbol{q} \cdot \boldsymbol{\lambda}_\tau \approx \boldsymbol{q} \cdot (\boldsymbol{\lambda} - \tau D^*\boldsymbol{\lambda}) , \quad (2)$$

the approximation following from a Taylor expansion. The changes in $\boldsymbol{q}$ of interest are those relative to $\mathbf{P}$ and can be deduced from an expression giving the rate of change of ξ. In the absence of collisions, ξ would be constant; collisions tend to drive ξ toward its equilibrium value of $\xi_1 \equiv \boldsymbol{q}_1 \cdot \boldsymbol{\lambda}_\tau$.

To simplify the model, we shall sort the collisions into groups, spaced at intervals of τ along the trajectory of $\mathbf{P}$, with ξ changing abruptly into ξ_1 at the end of each interval. Of course, such synchronous behavior is unreal but does not violate the essential physics. (A continuous version of the process is readily devised.) We may picture the property ξ as being swept along with the local thermodynamic system $\mathbf{P}$, persisting in value for a time τ and then being changed to ξ_1 by collisions. Suppose that at a time t, collisions have momentarily restored ξ to its equilibrium value $\xi_1(t)$, then in the absence of further collisions its magnitude will persist until time $(t + \tau)$ when it becomes the relative flux $\xi(t + \tau)$, at which instant collisions change it to $\xi_1(t + \tau)$. Thus,

$$\xi_1(t) = \xi(t + \tau) = \xi(t) + \tau D\xi + O(\epsilon^3) . \quad (3)$$

As ξ is proportional to $\boldsymbol{q}$, it is an $O(\epsilon)$ term; the operator τD is $O(\epsilon)$, making $\tau D\xi$ a second-order term.

The error in the second form of ξ given in equation (2) is $O(\epsilon^3)$, and therefore, since D is the same as D^* when applied to a scalar, equation (3) can be written as

$$\tau D^*[\boldsymbol{q} \cdot (\boldsymbol{\lambda} - \tau D^*\boldsymbol{\lambda})] + \boldsymbol{q} \cdot (\boldsymbol{\lambda} - \tau D^*\boldsymbol{\lambda})$$
$$= \boldsymbol{q}_1 \cdot (\boldsymbol{\lambda} - \tau D^*\boldsymbol{\lambda}) + O(\epsilon^3)$$

or

$$(\tau D^*\boldsymbol{q} + \boldsymbol{q}) \cdot \boldsymbol{\lambda} = \boldsymbol{q}_1 \cdot (\boldsymbol{\lambda} - \tau D^*\boldsymbol{\lambda}) + O(\epsilon^3) . \quad (4)$$

If we consider a short material line element $d\boldsymbol{x}$, namely, one that is convected with the fluid, then the rate of change of $d\boldsymbol{x}$ is the difference between the velocities at the two ends of the element. Hence, $D(d\boldsymbol{x}) = d\boldsymbol{x} \cdot \nabla \boldsymbol{v}$. In the mechanism described above, $\boldsymbol{\lambda}$ is a vector like $d\boldsymbol{x}$. Therefore, by the expansion $\nabla \boldsymbol{v} = \mathbf{e} - \boldsymbol{\Omega} \times \mathbf{1} = \dot{\mathbf{e}} - \boldsymbol{\Omega} \times \mathbf{1} + \frac{1}{3}\nabla \cdot \boldsymbol{v}\mathbf{1}$, where $\mathbf{1}$ is the unit tensor, we get $D\boldsymbol{\lambda} = \boldsymbol{\lambda} \cdot \nabla \boldsymbol{v} = \boldsymbol{\lambda} \cdot \mathbf{e} - \boldsymbol{\lambda} \times \boldsymbol{\Omega}$. Thus, $D\boldsymbol{\lambda} - \boldsymbol{\Omega} \times \boldsymbol{\lambda} \equiv D^*\boldsymbol{\lambda} = \boldsymbol{\lambda} \cdot \mathbf{e}$ is the rate of change of $\boldsymbol{\lambda}$ in the frame of the thermodynamic system $\mathbf{P}$. Therefore, as $\mathbf{e}$ is a symmetric tensor, $\boldsymbol{\lambda} - \tau D^*\boldsymbol{\lambda} = (\mathbf{1} - \tau \mathbf{e}) \cdot \boldsymbol{\lambda}$, allowing equation (4) to be written as

$$(\tau D^*\boldsymbol{q} + \boldsymbol{q}) \cdot \boldsymbol{\lambda} = \boldsymbol{q}_1 \cdot (\mathbf{1} - \tau \mathbf{e}) \cdot \boldsymbol{\lambda} + O(\epsilon^3) ,$$

and as this holds for all choices of $\boldsymbol{\lambda}$, we arrive at equation (1).

3. THE SECOND-ORDER HEATING MECHANISM, WITH MAGNETIC FIELD

We shall next generalize equation (1) to the case of a magnetoplasma. The charged particles circulate about the field lines with an angular velocity of $-\omega_c \boldsymbol{b}$, where ω_c is the cyclotron frequency and $\boldsymbol{b}$ is unit vector parallel to the magnetic field $\boldsymbol{B}$. Therefore, in a frame that accelerates and spins with the fluid *and* also gyrates with the particles, the total rate of change of the heat flux $\boldsymbol{q}$ is given by

$$\dot{\boldsymbol{q}} = D\boldsymbol{q} - \boldsymbol{\Omega} \times \boldsymbol{q} + \omega_c \boldsymbol{b} \times \boldsymbol{q} . \quad (5)$$

In order to calculate diffusion, it is essential to eliminate *all* ordered motions from the particles in the thermodynamic system $\mathbf{P}$. In a neutral gas, this is achieved by requiring $\mathbf{P}$ to accelerate and spin with the fluid element. In a magnetoplasma, by the same principle, it is necessary to allow for the collective motion of the particles about the lines of force; hence, from equation (5), it follows that in a magnetoplasma, equation (1) becomes

$$\tau D\boldsymbol{q} + (\boldsymbol{\varpi} - \tau\boldsymbol{\Omega}) \times \boldsymbol{q} + \boldsymbol{q} = \boldsymbol{q}_1^{(0)} - \tau \mathrm{e} \cdot \boldsymbol{q}_1^{(0)} , \qquad (6)$$

where

$$\boldsymbol{q}_1^{(0)} \equiv -\kappa \nabla T, \quad \kappa = 5k_{\mathrm{B}} p\tau/2m, \quad \boldsymbol{\varpi} \equiv \omega_c \tau \boldsymbol{b} ;$$

k_{B} is Boltzmann's constant, and m is the particle mass.

Setting $\boldsymbol{q} = \boldsymbol{q}_1 + \boldsymbol{q}_2 + O(\epsilon^3)$, we can rearrange equation (6) as

$$\tau D^* \boldsymbol{q}_1 + \boldsymbol{\varpi} \times (\boldsymbol{q}_1 + \boldsymbol{q}_2) + \boldsymbol{q}_1 + \boldsymbol{q}_2 = \boldsymbol{q}_1^{(0)} - \tau \mathrm{e} \cdot \boldsymbol{q}_{1(0)} ,$$

and separating this into first- and second-order terms, we get

$$\boldsymbol{\varpi} \times \boldsymbol{q}_1 + \boldsymbol{q}_1 = \boldsymbol{q}_1^{(0)}, \quad \boldsymbol{\varpi} \times \boldsymbol{q}_2 + \mathrm{q}_2 = -\tau \mathrm{e} \cdot \boldsymbol{q}_{1(0)} - \tau D^* \boldsymbol{q}_1 . \qquad (7)$$

The solution of the first of equations (7) is

$$\boldsymbol{q}_1 = \boldsymbol{k} \cdot \boldsymbol{q}_{1(0)} ,$$

$$\boldsymbol{k} \equiv \boldsymbol{bb} - \frac{\varpi}{1+\varpi^2}\, \boldsymbol{b} \times \boldsymbol{1} + \frac{1}{1+\varpi^2}\,(\boldsymbol{1} - \boldsymbol{bb}) . \qquad (8)$$

Similarly,

$$\boldsymbol{q}_2 = -\tau \boldsymbol{k} \cdot \mathrm{e} \cdot \boldsymbol{q}_1^{(0)} - \tau \boldsymbol{k} \cdot D^*(\boldsymbol{k} \cdot \boldsymbol{q}_1^{(0)}) . \qquad (9)$$

With strong magnetic fields ($\varpi \gg 1$) and no parallel gradients, $\boldsymbol{k} \approx -\boldsymbol{b} \times \boldsymbol{1}/\boldsymbol{\varpi}$, thus allowing us to reduce equation (9) to

$$\boldsymbol{q}_2 = -\tau \boldsymbol{k} \cdot \mathrm{e} \cdot \boldsymbol{q}_1^{(0)} \approx -\tau \boldsymbol{k} \cdot \dot{\mathrm{e}} \cdot \boldsymbol{q}_1^{(0)} = \frac{\tau}{\varpi}\, \boldsymbol{b} \times \dot{\mathrm{e}} \cdot \boldsymbol{q}_1^{(0)} .$$

Hence, our final expression is

$$\boldsymbol{q}_2 = -\frac{5k_{\mathrm{B}} p}{2QB}\, \tau \boldsymbol{b} \times \dot{\mathrm{e}} \cdot \nabla T , \qquad (10)$$

where Q is the particle electric charge. It applies to both the ion and electron gases and was first derived by a mean free path argument (Woods 1983).

We shall apply the theory to the case of a cylindrical magnetoplasma, with a strong, helical magnetic field, $\boldsymbol{B} = B_z \hat{z} + B_\theta \hat{\boldsymbol{\theta}}$, where $(\hat{r}, \hat{\boldsymbol{\theta}}, \hat{z})$ is the triad of unit vectors. It will be assumed that conditions are independent of the axial and azimuthal variables. Then $\nabla T = \hat{\boldsymbol{r}} T'$, where the prime denotes the radial derivative and the radial component of the second-order heat flux follows from equation (10):

$$Q_r \equiv \hat{\boldsymbol{r}} \cdot \boldsymbol{q}_2 = \frac{5k_{\mathrm{B}} p}{2QB}\, \tau_2 H T' , \qquad (11)$$

where $H \equiv \boldsymbol{b} \times \hat{\boldsymbol{r}} \cdot \dot{\mathrm{e}} \cdot \hat{\boldsymbol{r}}$.

For the unit vector parallel to $\boldsymbol{B}$, we have $\boldsymbol{b} = b_z \hat{z} + b_\theta \hat{\boldsymbol{\theta}} (b_z = B_z/B,\ b_\theta = B_\theta/B)$, where B is the field strength. The radial velocity v_r of either the ion or electron fluid is suppressed by the strong field to values much less than either the azimuthal component v_θ or the axial component v_z. With axial symmetry and uniform conditions along the axis, we find that

$$\nabla \boldsymbol{v} = v'_\theta \hat{\boldsymbol{r}} \hat{\boldsymbol{\theta}} - \frac{v_\theta}{r}\, \hat{\boldsymbol{\theta}} \hat{\boldsymbol{r}} + v'_z \hat{\boldsymbol{r}} \hat{z} ,$$

whence

$$H = \tfrac{1}{2}(v'_\theta - v_\theta/r) b_z - \tfrac{1}{2} v'_z b_\theta . \qquad (12)$$

Unlike the case with first-order heat flux, the radial heat flux in the electron gas is much larger than that in the ion gas. From equation (12) as applied to the electron gas ($Q = -e$), the radial heat flux is

$$Q_{e,r} = -\frac{5k_{\mathrm{B}} p_e}{2eB}\, \tau_{e2} H_e T'_e \quad \left[H_e = \frac{1}{2} r(v_{e\theta}/r)' b_z - \frac{1}{2} v'_{e,z} b_\theta\right] . \qquad (13)$$

The assumption that the electron and ion fluids have roughly the same momentum, i.e., that $v \propto m^{-1}$, allows us to simplify the expression for the current density, namely, $\boldsymbol{j} = en_e(\boldsymbol{v}_i - \boldsymbol{v}_e)$ to $\boldsymbol{j} = -en_e \boldsymbol{v}_e$, and write

$$H_e = -\frac{1}{2}\left[r\left(\frac{j_\theta}{ren_e}\right)' b_z - \left(\frac{j_\varphi}{en_e}\right)' b_\theta\right] .$$

Assuming equilibrium and negligible pressure, we have $0 = j_\theta B_z - j_z B_\theta$, which allows us to reduce the formula for H_e to

$$H_e = -\frac{\mu_0 j^2}{2en_e B} + \frac{j \sin 2\phi}{2en_e r} , \qquad (14)$$

where ϕ is the angle between $\boldsymbol{b}$ and $\hat{z}$. It now follows from equation (11) that the second-order radial heat flux is given by

$$Q_{e,r} = \frac{5k_{\mathrm{B}} p_e \tau_{en_e}}{(2en_e B)^2}\, \mu_0 j[j - B \sin 2\phi/(\mu_0 r)] T' . \qquad (15)$$

4. APPLICATION TO A CORONAL PLASMA LOOP

In cylindrical geometry, the total radial heat flux q_r follows by adding the second-order heat flux given by equation (15) to the standard expression for the first-order cross-field heat flux in the ion gas. (The cross-field flux in the electron gas can be ignored.) To simplify the account, we shall assume that $\delta_B/r \ll 1$, which means that the magnetic field changes over a distance that is small compared with the radius measured from the center of the flux tube (see Fig. 1). We find that

$$q_r = \left[\frac{5k_{\mathrm{B}} p_e n_e \tau_e}{(2en_e B)^2}\, \mu_0 j^2\right] \frac{\partial T}{\partial r} - \left(\frac{2k_{\mathrm{B}} p_i m_i}{e^2 B^2 \tau_i}\right) \frac{\partial T}{\partial r} , \qquad (16)$$

where the second term follows from Braginskii's treatment of the first-order transport in a magnetoplasma (Braginskii 1965). Let $\partial T/\partial r > 0$, so that the flux tube (called a "thread" below) is hotter than the ambient coronal plasma. From equation (1), we find that the heat will flow inward provided that

$$\frac{5n_e^2 \tau_e \tau_i}{8n_e^3 m_i}\, \mu_0 j^2 > 1$$

or

$$j > j_{\mathrm{cr}} , \quad j_{\mathrm{cr}} \equiv 2.16 \times 10^{-17} \ln \Lambda (n_e/T)^{3/2} , \qquad (17)$$

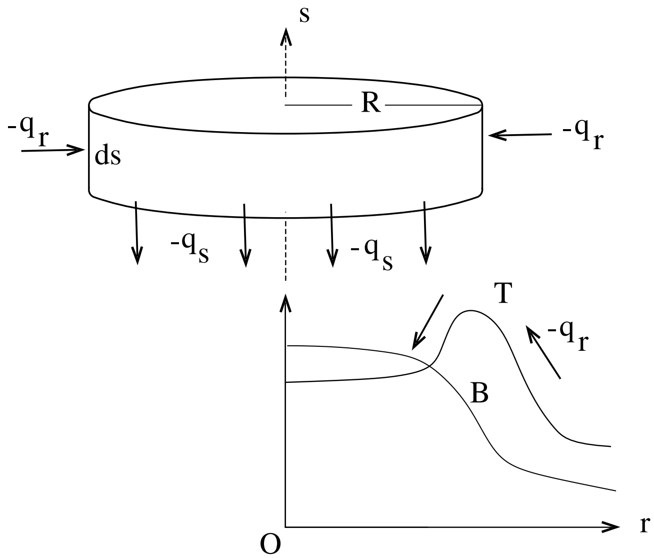

FIG. 1.—Temperature and magnetic field profiles

where

$$\ln \Lambda = 16.33 + 1.5 \ln T - 0.5 \ln n_e$$

is the Coulomb logarithm. In the following, we shall set $\ln \Lambda = 20$, which is a close approximation in all the thermodynamic conditions involved.

The maximum possible value for the current density, say, j_m, will occur when the electrons stream past the ions at the ion sound speed and the ion-acoustic instability sets in (see, e.g., Krall & Trivelpiece 1973, p. 477). Since the heating mechanism described above directly involves the electrons and since the rate at which the ions and electrons reach thermal equilibrium is relatively slow, we expect the instability to switch on when

$$j_m = en_e(k_B T/m_i)^{1/2} \approx 1.46 \times 10^{-17} P/T^{1/2} \quad (P \equiv n_e T) . \tag{18}$$

In hot loops, Bray et al. (1991, p. 157) give the typical values of $T = 2 \times 10^6$ K and $n_e = 5 \times 10^{15}$ m^{-3}, for which $j_{cr} = 5.4 \times 10^{-2}$ A m^{-2} and $j_m = 2.24 \times 10^2$ A m^{-2}, so heat could flow into the hot loops. On the other hand, with cool loops (e.g., $T = 2.1 \times 10^4$ K and $n_e = 5.6 \times 10^{16}$ m^{-3}), $j_{cr} = 1.88 \times 10^3$ A m^{-2} and $j_m = 1.13 \times 10^2$ A m^{-2}, so that the flow of heat up the radial temperature gradient is not possible.

The transition layer between the chromosphere and the corona has a temperature range of about 10^4–10^6 K in the middle of which (at $T \approx 10^5$ K) there is an abrupt change in the transport properties (Mariska 1992). We shall label this singularity M and measure the distance s along a thread upward from M. On the assumption that the magnetic field lies parallel to the axis of the thread, the heat is transported mainly by the electron gas, and, except in the neighborhood of M, its flux is given by (Braginskii 1965)

$$q_s = -\kappa \frac{\partial T}{\partial s} ,$$

$$\kappa = 3.16(k_B^2/m_e) T n_e \tau_e = \kappa_0 T^{5/2} \quad (\kappa_0 \approx 9.09 \times 10^{-12}) . \tag{19}$$

(Near M, observations of the differential emission measure suggest that turbulence modifies κ to something like $\kappa = \kappa_0 T^{5/2} + \kappa_2 T^{-5/2}$, with $\partial\kappa/\partial T \approx 0$ at M.)

If the condition in equation (17) is well satisfied, the radial heat flux is given by

$$q_r = \frac{5 k_B p_e n_e \tau_e}{(2 e n_e B)^2} \mu_0 j^2 \frac{\partial T}{\partial r} = \frac{2.031 \times 10^3 T^{5/2}}{n_e \ln \Lambda} \frac{1}{\delta_B^2} \frac{\partial T}{\partial r} \quad \left(\delta_B \equiv \frac{B}{\mu_0 j_m}\right) . \tag{20}$$

In this case, the thermal energy will tend to "pile up" in the neighborhood of $r = R$, as indicated in Figure 1, since at the top of the magnetic field profile where the current falls to zero, the heat flux will tend to reverse in direction, which will result in a local thermal instability. However, a temperature gradient will develop on the inside, and when this is steep enough, it will drive the heat further inward to heat the thread. But should it be the case that the inside (positive) temperature gradient is situated where a sufficiently strong current is flowing, the effect will be for the heat to flow outward from the inside, making the temperature peak stronger and leaving the thread with a cool core.

As the electrical conductivity is proportional to $T^{3/2}$, another effect of this local heating will be to concentrate the electric current in the region of the temperature peak, and ohmic heating will further increase the peak so that besides the thermal instability, there will be an associated current instability, and the current will increase to its maximum value given by equation (18). Since the temperature and electric current peaks will closely coincide, we can write $\delta_T \approx \delta_B$ for the temperature gradient scale length (see Fig. 1), where, by equation (18),

$$\frac{1}{\delta_B} = \frac{\mu_0 j_m}{B} = \frac{1.84 \times 10^{-23} P}{B T^{1/2}} .$$

Hence, with $\partial T/\partial r \approx -T/\delta_B$, equation (20) can be written as

$$q_r = -\frac{\kappa_1 P^2 T^3}{\ln \Lambda B^3} \quad (\kappa_1 = 1.25 \times 10^{-65}) , \tag{21}$$

where the B^{-3} dependence is a consequence of the three gradients involved in the second-order transport. The equivalent axial heating at the loop base (see § 1) is $Q_b = (2L/R) q_r$. With the values of $P = 2.17 \times 10^{21}$ K m^{-3}, $\ln \Lambda = 20$, $R/L \sim 0.05$, $T = 2 \times 10^6$ K, and $B = 2 \times 10^{-2}$ T (see Bray et al. 1991, p. 280), we find that $Q_b \sim 1.2 \times 10^2$ W m^{-2}, which is $\frac{1}{6}$ the value (7×10^2 W m^{-2}) measured by Svestka et al. (1977), but in view of the uncertainties in the values of B and the aspect ratio R/L, it appears that our mechanism could produce sufficient heating. In fact, with $B = 100$ G, the agreement between theory and observation is close. We also note from equation (21) that $q_r \propto n_e^2$, so the fact that the loops are rather denser than the ambient coronal enhances the inward flow of heat.

The heat supplied to the loop comes from the ambient corona, but we have not addressed the problem of how the corona itself gets heated. There will some dissipation due to the transport of heat across the magnetic field, but at this stage we accept that the required thermal energy near the boundary of the loop is derived from the radiation and conduction of energy from the more distant corona. The energy density of the corona is about an order of magnitude less than that in the loop, but its volume is vastly greater, so it is an adequate reservoir for our purpose. Its heating is a separate problem, our model being concerned just with the redistribution of this energy between loops and coronal plasma. Another point is that we have assumed the temperature of the loop to be greater than that of the corona. However, only a small difference is required to trigger the thermal instability, and once it starts growing, the temperature difference will increase, requiring energy to flow toward the loop from more distant coronal plasmas. We also note the possibility that if the loop is at a lower temperature than the ambient corona, the thermal instability will remove heat from the loop and cool it further, so long as the condition in equation (17) remains satisfied. We hope to pursue the question of cool loops in a later paper.

5. ENERGY EQUATION FOR A MAGNETIC THREAD

The energy balance for the unit length of the disk shown in Figure 1 is

$$\frac{\partial}{\partial t}(\pi R^2 \rho u) = -\frac{\partial}{\partial s}(\pi R^2 q_s) + \pi R^2(\mathscr{H} - \mathscr{L}) ,$$

where ρ is the density, u is the specific energy, $\mathscr{L}$ is the rate of energy loss per unit volume of the thread due to radiation, and $\mathscr{H}$ is the corresponding heating rate. In our case, $\mathscr{H}$ is not a volume-distributed energy supply but a surface term like $-\partial q_s/\partial s$ in a delta-function distribution at $r = R$. Energy is supplied radially to the disk at the rate of $-2\pi R q_r$, which is equivalent to a heating rate per unit volume of $-2q_r/R$.

We shall assume that the only sources of heating are due to the inward radial conduction described above and ohmic dissipation, so that

$$\mathscr{H} = -2\frac{q_r}{R} + \eta j^2(2\delta_B/R) \quad \left(\eta = \frac{0.51 m_e}{e^2 n_e \tau_e} \approx 65.8 \ln \Lambda T^{-3/2}\right) . \tag{22}$$

Evaluating the two terms in equation (22) for a typical thread, we find that the ohmic-heating term is negligible compared with the heating due to the inward radial flux; hence, we shall omit it.

For $\mathscr{L}$, we shall assume that the plasma in the thread (mainly hydrogen and helium) is singly and fully ionized; thus, if n_p is the number density of the radiating elements,

$$\mathscr{L} = n_e n_p Q(T) = P^2 Q(T)/T^2 \quad (P \equiv n_e T) ,$$

where the function $Q(T)$ is determined from theory. We shall adopt the approximation $Q(T) = aT^\gamma$ and select the constants a and γ so that $\mathscr{L} = 2 \times 10^{-2}$ W m^{-3} at $T = 10^5$ K and $\mathscr{L} = 2 \times 10^{-5}$ W m^{-3} at $T = 5 \times 10^6$ K, which are the values for the canonical hot loop model (see Bray et al. 1991, p. 280). The electron pressure for this model is $p_e = n_e k_B T = 3 \times 10^{-2}$ Pa, whence $P \approx 2.17 \times 10^{21}$ K m^{-3}. Thus, we find that

$$\mathscr{L} = aP^2 T^{\gamma - 2}$$

$$(a \approx 1.43 \times 10^{-33}, \gamma \approx -0.306, P \approx 2.17 \times 10^{21}) . \tag{23}$$

Let B_s denote the axial magnetic field and let us suppose that this is proportional to the total field B, then, by conservation of the magnetic flux along the loop, $\pi R^2 B_s$ is constant, whence $\mathscr{X} \equiv B/B_0 \propto 1/R^2$, where B_0 is a reference value of the field.

The energy equation now takes the form

$$\mathscr{X}\frac{\partial}{\partial t}\left(\frac{\rho u}{\mathscr{X}}\right) = \mathscr{X}\frac{\partial}{\partial s}\left(\frac{\kappa}{\mathscr{X}}\frac{\partial T}{\partial s}\right) + \frac{2\kappa_1 P^2 T^3}{R \ln \Lambda B^3} - aP^2 T^{\gamma - 2} . \tag{24}$$

The first two right-hand terms represent the convergence of heat in an element of the thread due to radial and axial conduction, and the last term is the loss of heat due to radiation. In the absence of a theory for the change in B along the flux tube, we shall assume that $\chi = 1$. With $\rho u = (3/2)p$, where p is the total pressure, which at any instant is assumed to have a constant value throughout the loop,[1] we can write equation (24) as

$$\frac{3}{2}\kappa\frac{\partial T}{\partial s}\frac{\partial p}{\partial t} = \frac{\partial}{\partial s}\left(\kappa\frac{\partial T}{\partial s}\right)^2 + 2\kappa(H_0 T^\beta - aP^2 T^{\gamma-2})\frac{\partial T}{\partial s} , \tag{25}$$

where

$$H_0 = \frac{2\kappa_1 P^2}{R \ln \Lambda B^3} , \quad \beta = 3 . \tag{26}$$

6. THE SCALING LAW

In Figure 2, we have sketched a coronal loop, which we have approximated by a segment of a torus with minor radius R and length $2L$. We have one obvious boundary condition, namely, that at $s = L$ where T has its maximum value T_m, the gradient $\partial T/\partial s$ is zero. Therefore, integrating the steady state form of equation (25) with the help of equation (19), we obtain

$$\frac{1}{2}\kappa_0 T^5\left(\frac{\partial T}{\partial s}\right)^2 = \frac{H_0}{\beta + 7/2}(T_m^{\beta + 7/2} - T^{\beta + 7/2}) - \frac{aP^2}{\gamma + 3/2}(T_m^{\gamma + 3/2} - T^{\gamma + 3/2}) . \tag{27}$$

To obtain a scaling law, i.e., to impose a constraint on the parameters, we need a further boundary condition. The sim-

[1] Although this assumption is commonly adopted, it should be remarked that it is not valid for large loops, which may extend over several hydrostatic scale heights.

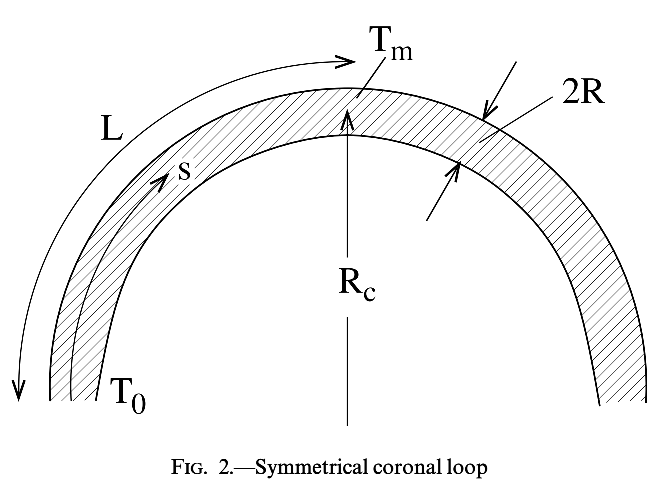

FIG. 2.—Symmetrical coronal loop

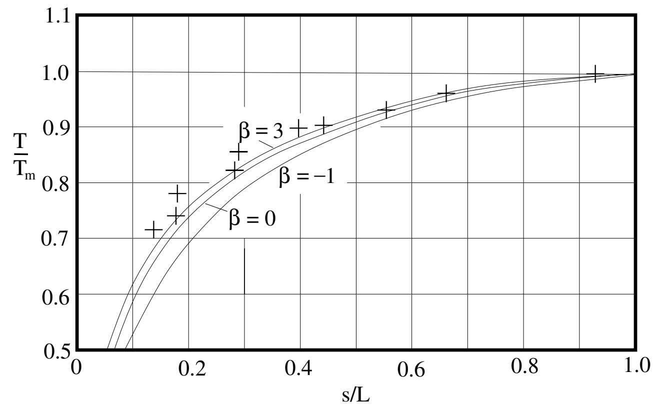

FIG. 3.—Temperature distributions

plest choice is to suppose that there is a temperature $T_0 \ll T_m$ at which the term on the left of equation (27) is negligible and can be omitted, which amounts to assuming that there is no conductive heat flux from the bottom of the loop (see, e.g., Bray et al. 1991). However, this requires a value of T_0 that falls in the low transition region where there is great uncertainty about both the thermal conductivity κ and the radiation function (Mariska 1992). Another approach is to choose a much higher value for T_0 and to evaluate equation (27) numerically, which is likely to be reasonably accurate in the upper transition zone. Hood & Priest (1979) followed this method, but with an empirical heating function proportional to the density, while Roberts & Frankenthal (1980) avoided the difficulty by neglecting radiation altogether.

Since our present purpose is to see how our new heating function compares with observation and the empirical proposals previously adopted, we shall follow the simplest model that yields a scaling law and set the left-hand side of equation (27) equal to zero when $T = T_0 \ll T_m$, which then requires that

$$H_0 = aP^2 \frac{\beta + 7/2}{\gamma + 3/2} T_m^{\gamma - \beta - 2} . \tag{28}$$

Now equation (27) yields

$$\frac{\partial T}{\partial s} = \left[\frac{2aP^2}{\kappa_0(\gamma + 3/2)}\right]^{1/2} T^{(1/2)\gamma - 7/4}\left[1 - \left(\frac{T}{T_m}\right)^{\beta - \gamma + 2}\right]^{1/2} . \tag{29}$$

Let

$$h = 2 + \beta - \gamma,\ l = \left(\frac{11}{4} - \frac{1}{2}\gamma\right)/h ,$$

$$g \equiv (T/T_m)^h,\ A = \left[\frac{2aP^2}{\kappa_0(\gamma + 3/2)}\right]^{1/2} ,$$

and as $g \approx 0$ at $s = 0$, the integral of equation (29) yields

$$s = \frac{T_m^{11/4 - (1/2)\gamma}}{hA} B\left(l, \frac{1}{2}\right) I_g\left(l, \frac{1}{2}\right) , \tag{30}$$

where $B(z, w) = \Gamma(z)\Gamma(w)/\Gamma(z + w)$ is the beta function and

$$I_x(z, w) = \frac{1}{B(z, w)} \int_0^x t^{z-1}(1 - t)^{w-1} dt$$

is the incomplete beta function.

At $s = L$, equation (30) yields the scaling law relating L and T_m (see, e.g., Bray et al. 1991),

$$PL = \left[\kappa_0\left(\gamma + \frac{3}{2}\right)\Big/ 2a\right]^{1/2} T_m^{11/4 - \gamma/2} B\left(l, \frac{1}{2}\right)\Big/ h , \tag{31}$$

where

$$B\left(l, \frac{1}{2}\right) = \sqrt{\pi}\,\Gamma\left(\frac{11 - 2\gamma}{8 + 4\beta - 4\gamma}\right)\Big/\Gamma\left(\frac{15 + 2\beta - 4\gamma}{8 + 4\beta - 4\gamma}\right) .$$

From equations (26) and (28),

$$\frac{2\kappa_1}{R \ln \Lambda B^3} = \frac{\beta + 7/2}{\gamma + 3/2} aT_m^{\gamma - \beta - 2} ; \tag{32}$$

hence,

$$R = \frac{\gamma + 3/2}{\beta + 7/2} \frac{2\kappa_1}{a \ln \Lambda} \frac{T_m^{5-\gamma}}{B^3} = 1.61 \times 10^{-34} T_m^{5.306} B^{-3} . \tag{33}$$

Typically, $T_m = 2 \times 10^6$ K and $B = 150$ G, whence $R = 128$ km. In this case, the total magnetic flux is $\Phi = \pi R^2 B = 4.2 \times 10^8$ Wb, which incidentally is close to the smallest observable element of magnetic flux and which Wang, Zirin, & Shi (1985) find is in the range of 10^8–1.4×10^9 Wb. An alternative expression for R follows on eliminating B in favor of Φ:

$$R = 2.58 \times 10^6 \Phi^{0.6} T_m^{-1.06} . \tag{34}$$

This is just the radius of a single thread, an assembly of which would be required to make up a typical hot plasma loop.

Following Galsgaard et al. (1999), we might hope to be able to discriminate between different heating models by comparing the temperature distribution each model generates with observation. From equations (30) and (32), we get

$$s/L = I_g\left(l, \frac{1}{2}\right)$$

$$[g = (T/T_m)^{2.306 + \beta},\ l = 2.903/(2.306 + \beta)] . \tag{35}$$

Figure 3 shows the distributions obtained with three values of β, but the distinction between $\beta = 3$ (our theory), $\beta = 0$ (uniform heating), and $\beta = -1$ (heating is greatest at the base of the loop) is less than the observation errors for the 10 points plotted in the figure, which are those reported by Priest et al. (1998). (In plotting these points, we have assumed the loop to be symmetrical and folded the points falling into $s > L$ back into the range $0 < s < L$.) It appears that our theory is marginally favored by the observations, but unfortunately the temperature distribution is too insensitive to the method of heating for a clear check on the theory.

7. CONCLUSIONS

We have introduced a method of heating plasma loops that depends on second-order heat transport across strong magnetic fields, a process that results in heat flowing *up* the temperature gradient. The energy is taken from the thermal energy in the ambient coronal plasma, so the theory does not immediately provide a solution for the problem of coronal heating. It does offer an explanation as to why some loops are much hotter than the corona and why cool loops are sometimes closely associated with hot loops. The heating rate is sufficient to balance the energy losses due to radiation and conduction along the plasma loop. We have found agreement with the observations of the temperature distribution along a small hot loop, but inaccuracies in these observations make it difficult for us to make clear distinctions between the various modes of heating that have been proposed. Thus, more observations are required to test the theory, which should next be extended to apply to the large cool loops studied by Aschwanden et al. (2000).

J. M. A. A. is supported by a Royal Society Dorothy Hodgkin Fellowship.

REFERENCES

Aschwanden, M. J., Nightingale, R. W., & Alexander, D. 2000, ApJ, 541, 1059
Aschwanden, M. J., Schrijver, C. J., & Alexander, D. 2001, ApJ, 550, 1036
Braginskii, S. I. 1965, in Reviews of Plasma Physics, Vol. 1, ed. M. A. Leontovich (New York: Consultants Bureau), 205
Bray, R. J., Cram, L. E., Durrant, C. J., & Loughhead, R. E. 1991, Plasma Loops in the Solar Corona (Cambridge: Cambridge Univ. Press)
Burnett, D. 1935a, Proc. London Math. Soc., 39, 385
———. 1935b, Proc. London Math. Soc., 40, 382
Craig, I. J. D., McClymont, A. N., & Underwood, J. H. 1978, A&A, 70, 1
Foukal, P., & Hinata, S. 1977, Sol. Phys., 132, 307
Galsgaard, K., MacKay, D. H., Priest, E. R., & Nordlund, Å. 1999, Sol. Phys., 189, 95
Heyvaerts, J., & Priest, E. R. 1983, A&A, 117, 220
Hinata, S. 1979, AJ, 232, 915
Hood, A. W., & Priest, E. R. 1979, A&A, 77, 233
Krall, N. A., & Trivelpiece, A. W. 1973, Principles of Plasma Physics (New York: McGraw-Hill)
Litvinenko, Y. E. 1999, Sol. Phys., 188, 115
Mariska J. T. 1992, The Solar Transition Region (Cambridge: Cambridge Univ. Press)
Neupert, W. M., Nakagawa, Y., & Rust, D. M. 1975, Sol. Phys., 43, 359
Priest, E. R., Foley, C. R., Heyvaerts, J., Arber, T. D., Culhane, J. L., & Acton, L. W. 1998, Nature, 393, 545
Reale, F., & Peres, G. 2000, ApJ, 528, L45
Roberts, B., & Frankenthal, S. 1980, Sol. Phys., 68, 103
Rosner, R., Tucker, W. H., & Vaiana, G. S. 1978, ApJ, 220, 643
Svestka, Z., Solodyna, C. V., Howard, R., & Levine, R. H. 1977, Sol. Phys., 55, 359
Wang, J., Zirin, H., & Shi, Z. 1985, Sol. Phys., 98, 241
Wentzel, D. G. 1981, Coronal Heating in the Sun as a Star, ed. S. Jordan (NASA SP-450; Washington, DC: NASA), 331
Woods, L. C. 1983, J. Plasma Phys., 21(1), 143
———. 1993, An Introduction to the Kinetic Theory of Gases and Magnetoplasmas (Oxford: Oxford Univ. Press)
———. 1996, Thermodynamic Inequalities with Applications to Gases and Magnetoplasmas (Chichester: Wiley)
Zirker, J. B. 1993, Sol. Phys., 148, 43